BILINGUAL PUBLISHING GROUP

Journal of Environmental & Earth Sciences

https://journals.bilpubgroup.com/index.php/jees

ARTICLE

Geological Characteristics and Preliminary Genesis Exploration of the Sakay Gold Deposit in Vientiane, Laos

Demin Yang [1], Chenming Liu [1*], Yuan Qin [2], Wei Huang [2], Nan Yang [2], Zheng Wang [1], Yungang Xiang [1]

[1] Institute of Resources and Environment, Yunnan Land and Resources Vocational College, Kunming 650093, China

[2] Yunnan Wuyan Technology Co., Ltd., Kunming 650091, China

ABSTRACT

The Sakay gold deposit in Vientiane, Laos, is located in the Indochina landmass of the southeastern segment of the Tethys orogenic belt, specifically within the Vientiane-Pakse micro-landmass and the Vientiane-Pakse metallogenic belt. This area is regionally significant for the concentration of minerals such as gold, copper, and tin. The host rocks of the deposit are intermediate volcanic lavas and volcanic tuffs, occurring in near-east-west brittle shear structural fractures through hydrothermal filling and metasomatism. The ore exhibits granular texture, subhedral texture, porphyritic texture, and oriented polycrystalline texture, with structural features such as disseminated, vein-like, and cataclastic breccia. The main ore minerals are pyrite, sphalerite, galena, and chalcopyrite, while the gangue minerals are primarily quartz, calcite, and dolomite. Gold is mainly present as included gold or fissure gold within the crystal lattices and microfractures of minerals such as pyrite and sphalerite. Based on mineral assemblages and generation timing, the mineralization can be divided into three stages: arsenopyrite-pyrite-dolomite-quartz (I), sphalerite-galena-chalcopyrite-calcite (II), and siderite (III), with the latter stages often overlaying the former, showing evident cross-cutting and metasomatic phenomena. The surrounding rocks in the mining area are altered, mainly showing silicification, carbonatization, limonitization, sericitization, and chloritization. Preliminary studies suggest that this deposit is a low-temperature hydrothermal gold deposit within a brittle shear zone.

Keywords: Laos; Gold Deposit; Hydrothermal; Porphyry; Brittle Shear

*CORRESPONDING AUTHOR:

Chenming Liu, Institute of Resources and Environment, Yunnan Land and Resources Vocational College, Kunming 650093, China; Email: xiao6yu2000@aliyun.com

ARTICLE INFO

Received: 21 January 2025 | Revised: 24 February 2025 | Accepted: 28 February 2025 | Published Online: 6 May 2025
DOI: https://doi.org/10.30564/jees.v7i5.8514

CITATION

Yang, D, Liu, C., Qin, Y., et al., 2025. Geological Characteristics and Preliminary Genesis Exploration of the Sakay Gold Deposit in Vientiane, Laos. Journal of Environmental & Earth Sciences. 7(5): 233–243. DOI: https://doi.org/10.30564/jees.v7i5.8514

1. Introduction

The Sakay Gold Mine is situated in the Sakai village, Sangthong District (M. Sangthong), Vientiane City, approximately 60 km southeast of the city center. Highway 11 passes through the western part of the work area. In the 1990s, relevant companies conducted mineral geological surveys and preliminary geological mappings in the region, discovering gold anomalies and mineralized bodies. Subsequently, other companies carried out large-scale geological investigations on the identified mineralized bodies, employing sparse trenching, drilling, and tunneling to expose and trace them. Exploration control and surface weathered ore body mining were also conducted on individual ore bodies. Despite some progress made in previous work, basic geological research in most parts of Laos remains inadequate. Many geological bodies lack evidence of geological age, and there is insufficient basis for their spatial distribution and correlation. The attributes of tectonic units have been a subject of debate[1–7], in particular, some geological bodies associated with large deposits have not been systematically studied[8–11], making it impossible to conduct systematic geological correlation research in the region. As a result, it is challenging to summarize the genesis and metallogenic patterns of regional deposits, let alone carry out large-scale metallogenic prediction and guide regional prospecting efforts. Recently, our team has conducted basic geological surveys and in-depth engineering explorations in the mining area, collected and analyzed a considerable number of rock and ore samples, and gained some fundamental geological insights and prospecting achievements. We have preliminarily determined the stratigraphic distribution and ore body characteristics in the mining area, clarified the mineralization stages, and tentatively proposed that the deposit is a low-temperature hydrothermal gold deposit associated with brittle shear zones. This article summarizes and organizes the metallogenic geological background, geological features of the mining area, and geological characteristics of the deposit, presenting an overview of the current geological work and research findings in the mining area. This is intended to provide technical guidance and a reference model for future deep geological prospecting work in the mining area and prospecting activities in the surrounding regions.

2. Data and Methods

2.1. Regional Geological Overview

The Sakay Gold Mine in Vientiane, Laos, is located in the Indochina Block, Vientiane-Pakse Microcontinent (III_2), in the southeastern segment of the Tethyan orogenic belt[12–18]. It belongs to the Vientiane-Pakse metallogenic belt, which is an important concentration area for minerals such as gold, copper, and tin in the region[19–21] (**Figure 1**). The stratigraphic sequences in the area are well-developed. From the Paleoproterozoic to the Early Paleozoic, they mainly consist of terrigenous clastic sediments containing carbonate rocks and intermediate-basic volcanic rocks, primarily deposited in a passive continental margin setting. From the Devonian to the Middle Triassic, they are mainly carbonate rocks containing volcanic rock series. In the Middle-Late Permian, terrigenous clastic sediments containing coal developed. The Indosinian movement lifted the region, ending the history of marine deposition and initiating the evolution of inland deposition. It also caused the collision between the Vientiane-Pakse Microcontinent (III_2) and the Northeast Truong Son Microcontinent (III_3), resulting in intense collisional volcanic activity in the region. The Yanshanian movement transformed the regional tectonic framework, with compression stresses mainly in the NE-SW direction, shaping the NW-trending tectonic distribution in the area and developing a series of faulted basins. Locally, intermediate-acidic magmatic intrusions occurred. During the Himalayan period, the region experienced uneven uplift, with the development of inland river and lake sediments, and locally, basic volcanic activity. The regional tectonic style is relatively uniform, mainly characterized by NW-trending fault structures, while fold structures are not well-developed. Magmatic activity is frequent, mainly dominated by intermediate-acidic volcanic lavas and volcaniclastic rocks, with local occurrences of intermediate-acidic intrusive dikes.The regional basic geological survey work is inadequate, lacking systematic research and comparison. Based on current understanding, the work area mainly exposes late Paleozoic to Early Triassic intermediate volcanic rocks and acidic intrusive rocks, Middle to Late Triassic intermediate-acidic volcanic rocks and intrusive rocks, as well as Late Triassic to Jurassic sedimentary clastic rocks and Quaternary alluvial-pluvial deposits.

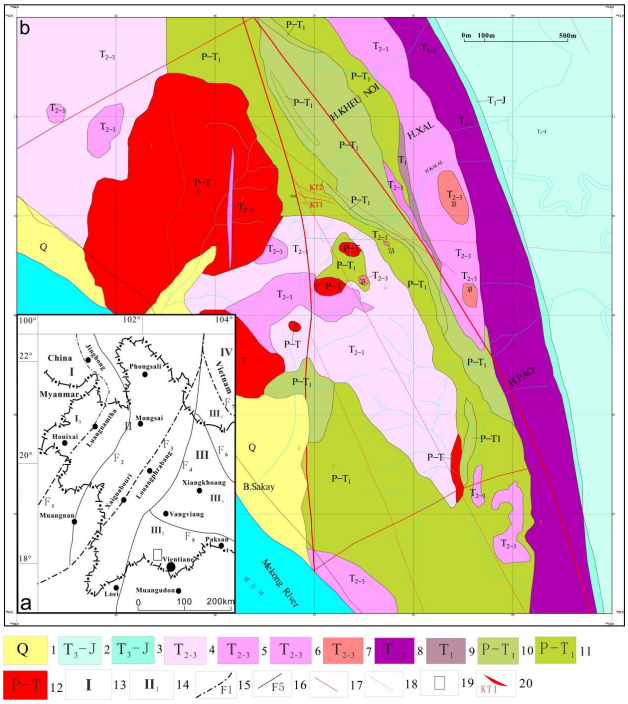

Figure 1. Geological sketch of the working area: (**a**) regional structural framework map; (**b**) geological sketch of the mining area.

Note: 1—Quaternary alluvium; 2—Upper Triassic-Jurassic siltstone; 3—Upper Triassic-Jurassic sedimentary conglomerate; 4, 5, 6—Middle-Lower Triassic rhyolitic volcanic lava, tuff; 7—Middle-Lower Triassic granodiorite; 8—Middle-Lower Triassic red siltstone; 9—Lower Triassic siliceous rocks (chert) layer; 10—Lower Triassic-Permian volcaniclastic rocks, breccia; 11—Lower Triassic-Permian andesitic volcanic rocks, volcanic tuff; 12—Lower Triassic-Permian granite porphyry; 13—Continental blocks and their numbers; 14—Microcontinental blocks and their numbers; 15—Faults delineating continental block boundaries; 16—Regional faults; 17—Faults within the mining area; 18—Inferred faults within the mining area; 19—Location of the mining area; 20—Location of gold ore bodies and samples. **Figure 1a** is modified based on [17].

Based on the regional tectonic framework map (**Figure 1a**) and previous studies [22, 23], the study area is located in the southwestern part of Laos, extending in a northwest-trending belt. It is situated within the Vientiane-Pakse microcontinent (III_2) of the Indochina Block in the southeastern segment of the Tethyan orogenic belt. The area is bounded by the F_4 Phu Pulei Fault to the northwest and the F_5 Truong Son-Da Nang Fault to the northeast, extending south and southwest into neighboring countries. The tectonic features within the area are predominantly northwest-trending fault structures, with folds being relatively underdeveloped. The F_4 Phu Pulei Fault extends in a northeast direction, stretching over 300 kilometers within the study area. It serves as the boundary fault between the Luang Prabang Island Arc Belt (III_1) and the Vientiane-Pakse microcontinent (III_2). Along this fault, a strong structural melange zone is developed, with suspected tectonic ophiolite melange in the northern segment of the fault. In the later stages of fault activity, it exhibited dextral strike-slip movement, causing northeast-directed shear on the western side of the adjacent tectonic framework and northwest compression on the eastern side. The F_5 Truong Son-Da Nang Fault is located on the western slope of the Truong Son Mountains in southeastern Laos, extending northwest for 700 kilometers. It serves as the boundary fault between the Vientiane-Pakse microcontinent (III_2) and the Truong Son microcontinent (III_3). To the southeast of the fault, there is stable and continuous deposition, while to the northeast, Hercynian and Indosinian intermediate-acidic volcanic rocks are developed. This fault may represent a deep major fault zone controlling regional volcanic and magmatic activities.

2.2. Geological Characteristics of the Ore Deposit

The mining area is mainly exposed to late Paleozoic to Early Triassic intermediate volcanic rocks and Middle to Late Triassic felsic volcanic rocks, with most regions covered by volcanic lavas and volcaniclastic rocks. The fault structures within the area are well-developed, predominantly striking northwest in alignment with the regional main structural trend. Based on field geological surveys, it is preliminarily inferred that the ore bodies occur within a set of northwest-striking brittle shear zones. The fault to the east functions as the ore-controlling fault, representing a sinistral strike-slip fault. The ore bodies are primarily hosted in secondary fault zones developed in near-east-west orientations within intermediate volcanic lavas and volcanic tuffs, intersecting with the northwest-striking faults.

2.2.1. Characteristics of Ore Bodies

Based on current exploration work, two industrial ore bodies (**Figures 2–4**) have been delineated in the mining area, as described below:

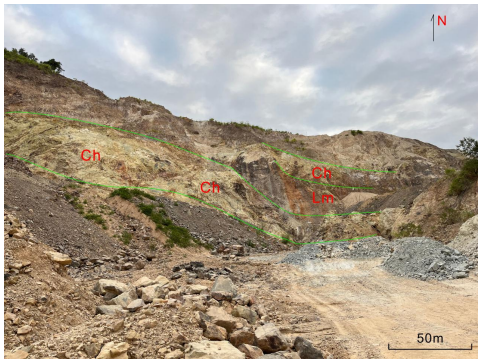

Figure 2. Open-pit mining face of orebody KT1.

Note: Ch, chloritization; Lm, limonitization.

Ore Body KT1: The ore body extends approximately 300 meters along strike, with a dipping depth of about 200 meters. It has a thickness of 0.3–1.5 meters and a grade of 1.6–43.6 g t^{-1}. It trends gently towards the south with dips of 30°–40°, reaching a maximum of 50°. It exhibits characteristics of steeper dips in the shallow parts and gentler dips in the deeper parts, as well as steeper dips in the west and gentler dips in the east. The ore body is distributed in a near-east-west direction along the fault zone, pinching out towards the east in an east-northeast direction and gradually pinching out towards the west. It is strictly controlled by the fault zone and has a lenticular shape, with local enlargement, narrowing, pinch-out and reappearance, and branching and composite features.

Ore Body KT2: The ore body extends approximately 280 meters along strike, with a dipping depth of about 200 meters. It has a thickness of 0.2–0.8 meters, with an average thickness of 0.4 meters, and a grade of 3.56–8.8 g t^{-1}. It trends towards the southwest with dips of 40°–50°, reaching a maximum of 60°. It exhibits characteristics of gentler dips in the shallow parts and steeper dips in the deeper parts, as well as steeper dips in the west and gentler dips in the east. The ore body is distributed in a near-east-west direction along the fault zone, approximately parallel to KT1. It pinches out towards the east in an east-southeast direction and gradually pinches out towards the west. It is strictly controlled by the fault zone and has a lenticular shape, with pinch-out and reappearance, and branching and composite features.

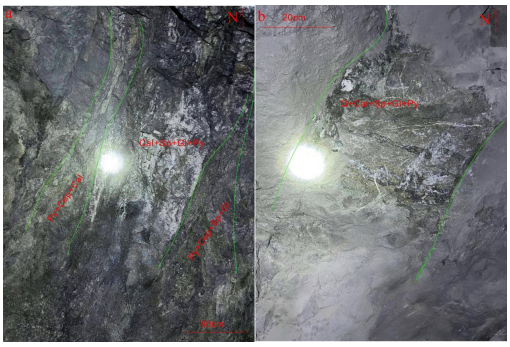

Figure 3. Images inside the pit of orebody KT1: (**a**) underground mining face of orebody, and (**b**) silicified and carbonatized disseminated and vein-like ore.

Note: Py, Pyrite; Sp, Sphalerite; Gl, Galena; Ccp(Cep), Chalcopyrite; Q, Quartz Silicification; Cal, Carbonatization. (**a**) The mining face primarily consists of hydrothermal fill-metasomatic veins within structural fracture zones. The veins are approximately 1.2 m in width, trending towards the southwest, with an inclination of around 50°. The ore primarily exhibits brecciated and agglomerated textures due to silicification and carbonatization. The fracture zones near the walls are mainly composed of sparsely disseminated sulfide ores with silicification, while the center contains strongly carbonatized cemented brecciated ore. (**b**) The silicified ore veins or ores are notably intersected and filled by carbonate veins. The silicification and carbonatization processes have resulted in a disseminated and vein-like ore texture.

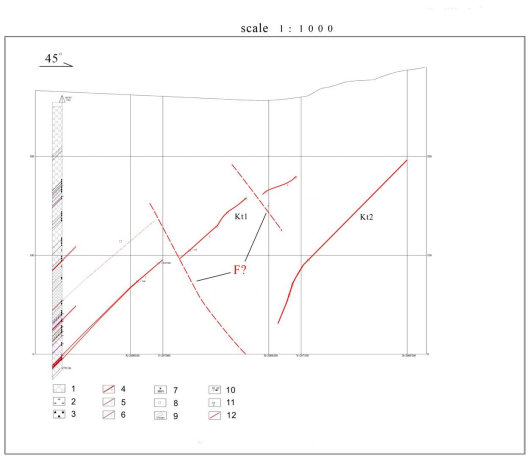

Figure 4. Typical exploratory line profile of orebody.

Note: 1 Acidic Volcanic Lava;2 Granite Porphyry Volcanic; 3 Breccia Lava; 4 Orebody and Number; 5 Low-Grade Orebody; 6 Gold Mineralized Vein;7 Boreholes and Numbers (Plan View); 8 Tunnels (Profile View); 9 Tunnels and Numbers (Plan View); 10 Samples; 11 Occurrence (Geological Attitude); 12 Faults (Dashed Lines Indicate Inferred Faults).

Based on field geological surveys and exposure of surface and underground ore bodies, it is speculated that the ore bodies may originate from a set of left-lateral brittle shear zones, with the ore bodies confined to tension-compression fracture zones formed by these brittle shear zones.

2.2.2. Characteristics of Ore

The main types of ore in the ore bodies include surface-weathered limonite, quartz vein (silicified) sulfide, and carbonatized sulfide. Gold primarily occurs as lattice gold (included gold) and fissure gold within sulfides or oxides. The main ore minerals include pyrite, galena, sphalerite, limonite, arsenopyrite, siderite, and a small amount of chalcopyrite. The main gangue minerals include quartz, dolomite, and calcite (**Figure 5**). The main textures of the ore include crystalline, microporous, inequigranular, subhedral, cataclastic, and porphyritic-oriented crushed textures. The main structures include veinlet, breccia, lenticular, and disseminated structures.

2.2.3. Wall Rock Alteration

Wall rock alteration is well-developed in the ore deposit, mainly including silicification, carbonatization, sericitization, chloritization, and limonitization. Based on surface and underground exploration work, it can be roughly divided into: mineralization-alteration zones characterized by silicification and carbonatization; near-ore wall rock alteration zones characterized by chloritization and sericitization; and surface weathering alteration zones characterized by limonitization.

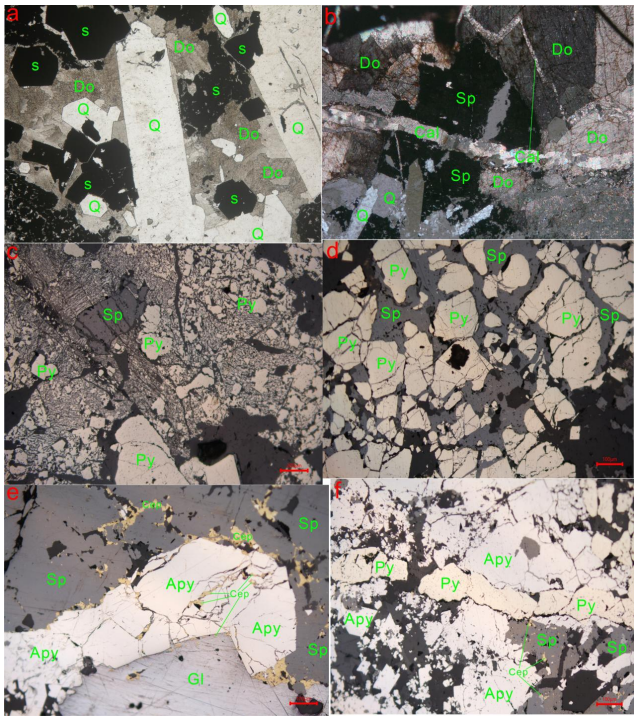

Figure 5. Polarizing microscope plates of ore minerals. (**a**) Euhedral quartz (Q) and dolomite (Do) in sulfide (S), plane-polarized light, 100×; (**b**) Sphalerite (Sp) cut by calcite (Cal) veins, cross-polarized light, 100×; (**c**) Mosaic-like crushed structure of pyrite (Py), with gray sphalerite (Sp) grains containing fragmented pyrite (Py) particles, plane-polarized light; (**d**) Pyrite (Py) cemented or veined by sphalerite (Sp), plane-polarized light; (**e**) Galena (Gl), chalcopyrite (Ccp/Cep), and sphalerite (Sp) distributed along fractures in arsenopyrite (Apy), forming intersecting veinlet-stockwork structures; chalcopyrite also intersects and replaces sphalerite, plane-polarized light; (**f**) Fine veins of pyrite (Py) cutting through arsenopyrite (Apy); gray areas are sphalerite (Sp) containing chalcopyrite (Ccp/Cep) and galena (Gl), plane-polarized light.

Based on extensive collection and summary of previous work, combined with the current mining area activities, we have adopted methods such as observing geological points and routes at certain intervals, measuring typical geological sections, and identifying rock and ore samples under a microscope. These methods and means have been used to conduct detailed investigations and studies on geological information including strata, rocks, ore bodies, wall rock alterations, and structural distributions. With the limited information resources currently available, we aim to summarize the geological characteristics of the ore deposit and explain its genesis.

3. Results and Analysis

3.1. Stratigraphic and Lithological Characteristics

3.1.1. Late Paleozoic to Early Triassic Intermediate-Acidic Volcanic Rocks and Intrusive Rocks

Granite Porphyry (**Figure 6**): It exhibits a light flesh-red hue and is mostly exposed as small rock stocks on the surface. The rock is strongly weathered and heavily argillized. It has a porphyritic texture with a microgranular matrix. The rock is composed of phenocrysts and matrix. The phenocrysts, which account for 5 to 10% of the rock, are euhedral granular quartz, orthoclase, and plagioclase. The matrix is composed of microgranular felsic minerals and very little biotite, exhibiting a porphyritic and microgranular texture. Quartz: It is colorless and occurs as phenocrysts and in the matrix. The phenocrysts are euhedral, isometric, and corroded, containing biotite inclusions. The matrix quartz is microcrystalline and granular, accounting for 30 to 35% of the rock. Orthoclase: It is colorless and has a dirty surface, occurring as phenocrysts and in the matrix. The phenocrysts are mostly euhedral tabular and show Kasperbauer twins under crossed polars, and they have undergone argillization. Plagioclase: It is colorless and occurs as phenocrysts and in the matrix. The phenocrysts are euhedral tabular to prismatic and show albite twins and sodium-feldspar twins (twinned on 100) under crossed polars. Biotite: It occurs as flakes and strips in the matrix and is present in very small quantities.

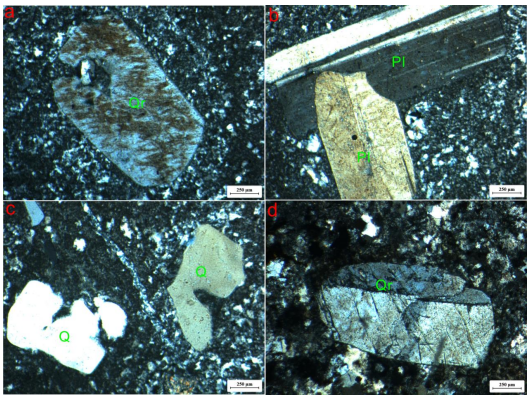

Figure 6. Plate of granitic porphyry orthogonal polarized light 50×. (**a**) Porphyritic texture with clay-altered orthoclase (Qr) phenocrysts distributed in a felsic matrix; (**b**) Porphyritic texture with plagioclase (Pl) phenocrysts distributed in a felsic matrix; (**c**) Porphyritic texture with corroded quartz (Q) phenocrysts distributed in a felsic matrix; (**d**) Porphyritic texture with orthoclase (Or) phenocrysts distributed in a felsic matrix.

Andesitic crystal-vitric plastic lapilli tuff (**Figure 7**) exhibits a grayish-brown hue and displays a welded tuff texture with plastic deformation and pseudoflow structures. The rock is composed of andesitic volcanic clasts and basement (or debris from the volcanic conduit). The volcanic clasts, accounting for more than 80% ± of the rock, are composed of plastic lapilli, crystal fragments, plastic vitric fragments, and volcanic ash. The plastic lapilli are molten masses composed of intermediate vitric material, generally larger than 2 mm, and may contain phenocrysts, microcrystals, vesicles, amygdales, etc. They often occur in flame-tongue, pancake, lenticular, branched, and banded shapes. The crystal fragments are all plagioclase, which are phenocrysts crystallized early in the magma and fragmented during volcanic eruptions, belonging to the same source component. Vitric fragments refer to vitric debris less than 2 mm to 0.02 mm in size, often occurring in flame-tongue, lenticular, arcuate, polygonal with curved surfaces, Y-shaped, and torn shapes. The volcanic ash consists of dust-like glass particles smaller than 0.02 mm, occurring as vein fillings. When the volcanic clasts were in a high-temperature plastic state, they were flattened into lenticular shapes. The vitric fragments and volcanic ash underwent welding, and the plastic vitric fragments were wave-like and orientationally arranged around the crystal fragments, forming pseudoflow structures. The basement rocks are composed of quartz crystal fragments, granite porphyry fragments, and felsic matrix, accounting for 15 to 20% of the rock. Due to later stress, the rocks show crushing, and quartz aggregates of varying crystallinity fill the fractures.

3.1.2. Intermediate-Acidic Volcanic Rocks and Intrusive Rocks of the Middle to Late Triassic

Rhyolitic tuff lava exhibits a grayish-brown to light flesh-red hue, with a porphyritic and felsitic texture. The rock is composed of phenocrysts, matrix, and crystal-vitric tuffaceous material (**Figure 8**). The phenocrysts, accounting for approximately 40% ± of the rock, are mainly quartz and plagioclase. Some of the quartz and plagioclase phenocrysts are fragmented due to decompression during ascent, forming angular crystal fragments (i.e., autoclastic debris) distributed within the felsitic matrix. Plagioclase occurs as phenocrysts and mostly as angular crystal fragments. Under crossed polars, albite twins are visible, but most of the plagioclase has been sericitized, accounting for 30 to 35% of the rock. Quartz is colorless and occurs mainly as phenocrysts and secondarily as angular crystal fragments, with a small amount distributed in the matrix. The phenocrysts are euhedral, isometric, fragmented, and corroded, while the crystal fragments are angular to sharply angular. In the matrix, quartz is microcrystalline, with low positive relief and a first-order pale yellow interference color under crossed polars, accounting for 25 to 30% of the rock. Orthoclase occurs as felsitic material distributed within the matrix, with very weak optical properties, accounting for approximately 35% ± of the rock.

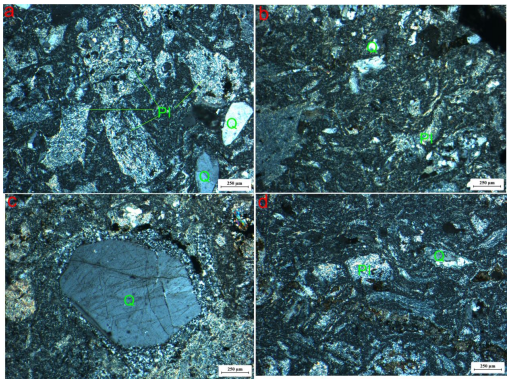

Figure 7. Andesitic crystal-fragment and plastic-deformed lithic-fragment weld tuff orthogonal polarized light, 50×. (**a**) Palimpsest crystal-fragment tuff texture, with crystal fragments being altered plagioclase (Pl) and a small amount of quartz (Q), cemented and filled by volcanic ash and glass shards; (**b**) Marginally altered glass shard muddification texture, pseudoflow texture, with devitrified glass shards showing wavy, oriented arrangement (weak welding); (**c**) Lithic muddification texture, with granite porphyry fragments and a small amount of altered plagioclase (Pl) crystal fragments distributed within the cement of volcanic ash and glass shards; (**d**) Pseudoflow texture, formed by altered plastic-deformed glass shards, with a small amount of quartz (Q) and plagioclase (Pl) crystal fragments arranged in a wavy, oriented manner.

Diorite (**Figure 9**) exhibits a light grayish-green hue and a euhedral fibrolitic-granular texture. The rock is primarily composed of amphibole, plagioclase, and a small amount of magnetite. Amphibole occurs as long, fibrolitic columns distributed chaotically, with its framework filled by subhedral fine-grained equiaxial plagioclase grains, forming a fibrolitic-granular texture. Amphibole: Yellowish-green in color, euhedral and long columnar in shape. The cross-section may appear rhomboidal or hexagonal, though this is not well-developed. It exhibits clear pleochroism, ranging from yellow-green to light green. It has high positive relief and two sets of rhomboidal cleavage. Under crossed polars, it displays a brown anomalous interference color

and exhibits oblique extinction. Plagioclase: Colorless and subhedral fine-grained equiaxial grains. Under crossed polars, it exhibits albite twins. However, it has undergone varying degrees of sericitization and carbonatization. The maximum extinction angle Np'□(010) measured on a few residual grains perpendicular to the (010) cleavage plane is 27°, with an An content of 50%. Magnetite: Black and opaque, with euhedral to subhedral quadrangular shapes. It exhibits a metallic sheen that is iron-black under reflection. Its content is ≤1%.

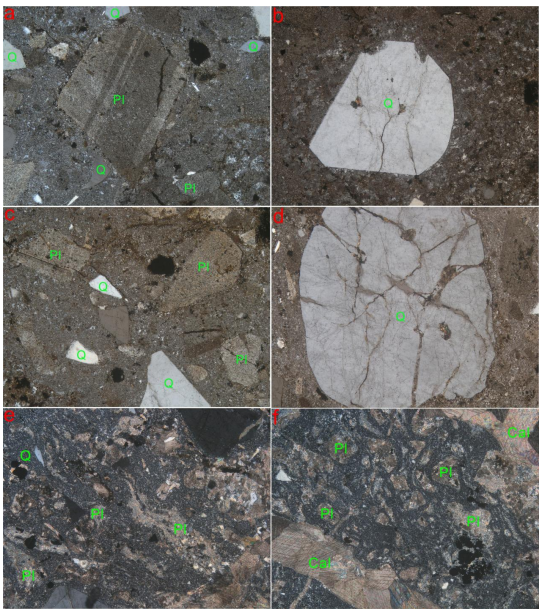

Figure 8. Plate of rhyolitic tuff lava under crossed polarized light, 100×. (**a**) Porphyritic texture with a felsic phyric groundmass, phenocrysts including sericitized plagioclase (Pl) and a small amount of quartz (Q) crystal fragments; (**b**) Porphyritic texture with a felsic phyric groundmass, phenocrysts being subhedral corroded quartz (Q); (**c**) Crystal-lava texture, angular quartz (Q) and sericitized plagioclase (Pl) distributed within the felsic phyric groundmass; (**d**) Cataclastic porphyritic texture, euhedral cataclastic quartz (Q) phenocrysts distributed within the felsic phyric groundmass. (**e**) Flow texture with sericitized plagioclase (Pl) crystal fragments oriented within a felsitic groundmass, reflecting the flow characteristics of the magma; (**f**) Crystal-tuff lava texture, where plagioclase (Pl) phenocrysts are fragmented into angular crystal fragments due to explosion and distributed within a felsitic groundmass, with Cal representing secondary calcite.

Altered Diorite Porphyry (**Figure 10**) exhibits a grayish-green hue, with a relict porphyritic texture and a relict microcrystalline platy-prismatic texture in the matrix. The rock is composed of phenocrysts and matrix. The phenocrysts are predominantly short-prismatic altered amphiboles, with very few plagioclases, accounting for 5 to 10% of the rock. The matrix consists of euhedral platy-prismatic microcrystals of plagioclase and a small amount of dust-like iron oxides, exhibiting relic porphyritic and relic microcrystalline platy-prismatic textures. Plagioclase: Occasionally occurring as phenocrysts, it mainly occurs as platy-prismatic microcrystals and has been completely replaced by sericite. Main altered dark minerals: Amphibole, light green in color and short-prismatic in shape, with equiaxial granular cross-sections. It has been completely replaced by chlorite and iron oxide or has been leached out leaving voids, accounting for approximately 15% ± of the rock. Iron oxides: Black and dust-like in appearance.

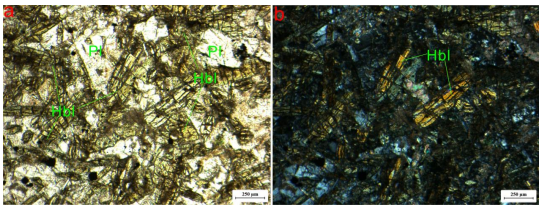

Figure 9. Diorite plate. (**a**) Semi-idiomorphic fibrous-prismatic granular texture, composed of semi-idiomorphic hornblende (Hbl) and prismatic plagioclase (Pl) with a small amount of magnetite, in plane-polarized light, 50×; (**b**) Semi-idiomorphic fibrous-prismatic granular texture, composed of semi-idiomorphic hornblende (Hbl) and prismatic plagioclase (Pl) with a small amount of magnetite, in cross-polarized light, 50×.

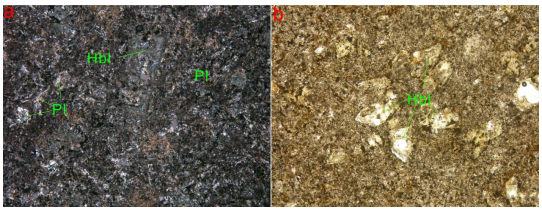

Figure 10. Altered dioritic porphyry. (**a**) Relict Porphyritic Texture, with phenocrysts of chloritized Diorite (Hbl) distributed within a matrix of sericitized prismatic plagioclase (Pl) and quartz (Q) microcrystals. Orthogonal polarized light, 100×; (**b**) Relict Poikiloblastic Texture, where the relict poikiloblasts are aggregated chloritized Diorite (Hbl). Plane polarized light, 100×.

3.2. Ore-Forming Processes and Mineralization Stages

Based on field observations of geological points and routes, indoor identification using optical and thin section microscopy, as well as exploration engineering controls, and in conjunction with the macroscopic distribution of the ore bodies and the microscopic characteristics of the rocks and ores, this paper speculates that the ore deposit is primarily formed through hydrothermal filling-metasomatic mineralization, the metallic minerals composing the ore include

arsenopyrite, pyrite, sphalerite, galena, chalcopyrite, and siderite. The gangue minerals constituting the ore mainly include quartz, dolomite, and calcite. According to the mineral assemblage and temporal relationships, the mineralization period can be divided into three stages: arsenopyrite-pyrite-dolomite-quartz (Stage I), sphalerite-galena-chalcopyrite-calcite (Stage II), and siderite (Stage III). The latter stages often overlay the former, with obvious interpenetration and metasomatism phenomena. In Stage I mineralization, pyrite can be seen as veins cutting through arsenopyrite, indicating that arsenopyrite formed earlier than pyrite. Due to tectonic activity, arsenopyrite and pyrite are mostly fragmented, with chalcopyrite, galena, and sphalerite distributed in the fractures, often forming cross-veined and reticulated structures. Quartz through dolomite fracture cleavages, reflecting that dolomite precipitated earlier than quartz. In Stage II mineralization, sphalerite is commonly and metasomatized by chalcopyrite and galena in veins, indicating that sphalerite formed earlier than chalcopyrite and galena. Chalcopyrite simultaneously metasomatizes galena, which formed later. Meanwhile, calcite veins obviously through sphalerite and fill and cement breccia-type sulfides. The third type of bands has the characteristic of cutting through the second type of bands, and the bands contain sphalerite fragments. Under polarized light, pyrite exhibits crushed spotty, mottled, and oriented pressure-fission crystalline structures, reflecting strong compressive stress characteristics. This may indicate that both the tectonic stress background field and ore-forming fluids underwent significant changes after the first stage of mineralization, clearly shifting towards compressive stress and fluids rich in CO_3^{2-} ions and lead-zinc ions. The abundance of Mg^{2+} and Ca^{2+} in the host rocks of moderately acidic volcanic lavas and volcanic tuffs provided the material composition and chemical environment for hydrothermal metasomatism, facilitating the precipitation and deposition of gold and gold-bearing minerals, and forming intense carbonate and chloritization alteration zones in the surrounding rocks near the ore deposit.

4. Discussion

Many scholars have conducted relevant research on the geological characteristics of gold deposits in Laos and attempted to summarize the metallogenic regularities [24, 25]. Currently, it is mainly believed that the gold deposits within the Truong Son metallogenic belt in Laos were formed during the Late Carboniferous to Early Permian, while those within the Loei metallogenic belt were formed during the Late Permian to Early-Middle Triassic [26]. Additionally, the source of gold material has not been discussed. The metallogenic epoch of the deposit and related issues will be studied and discussed in subsequent papers.Based on the geological characteristics of the ore deposit, combined with studies of ore body distribution and ore assemblage patterns, it is believed that the ore deposit is a low-temperature hydrothermal filling-metasomatic gold deposit produced in brittle shear zones.The ore deposit is strictly confined and occurs within fault structures, and it does not have a direct genetic relationship with the widespread volcanic activity in the region. It shares similar ore-controlling characteristics with gold deposits in the Ailaoshan area of Yunnan, southwestern China, and the Jiaodong area of Shandong, China [27, 28], all of these deposits are significantly controlled by fault structures, however, the ore deposit studied in this research is predominantly controlled by brittle shear structural fractures, whereas the gold deposits in the other two regions are controlled by ductile shear zones in their respective areas.In terms of the sources of gold, sub-basic volcanic rocks are considered significant contributors to the gold deposits in the Ailaoshan region of Yunnan and the Jiaodong region of Shandong. Currently, it is believed that sub-acidic porphyry may be an important source of gold material for this type of ore deposit. More formally, the analysis in this paper suggests that tectonic activity during the Hercynian and earlier periods resulted in widespread intermediate-basic magmatic activity, which may have constituted the material basis and abundant hydrothermal fluids for gold,during the Indosinian movement, intense collisional orogeny accompanied by intermediate-acidic volcanic magmatic activity, coupled with regional tectonic transformation, formed a northwest-trending structural pattern and compressive-shear-tension fracture zones in the mining area, providing space for the ascent of hydrothermal fluids and the emplacement of ore bodies,moderately acidic volcanic lavas and volcanic tuffs provided the chemical environment for hydrothermal metasomatism and the precipitation and deposition of gold and gold-bearing minerals, in the late Indosinian period, intermediate-acidic porphyry intrusions, mixed with multiple episodes of volcanic hydrothermal flu-

ids, continuously extracted and activated gold from earlier magmatic activity and gold carried within themselves, under the background of regional compressive-shear stress, they ascended into the underpressured brittle shear zones and formed gold ore bodies through filling-metasomatism.

Currently, the mining area is simultaneously carrying out prospecting and exploration work in the directions of the ore body's dipping extension, strike extension, and the surrounding areas. The revelation of the ore deposit's genesis, metallogenic regularities, and main ore-controlling factors will directly influence the prospecting methods and exploration directions for this mine and the surrounding mines. If, as analyzed in this paper, the ore deposit is a low-temperature hydrothermal filling and replacement gold deposit in brittle shear zones, strictly controlled and occurring within fault structures, then the subsequent prospecting work in the mining area will be organized around the ore-controlling faults, with fault structures being the primary target for prospecting efforts in their distribution areas. If the ore deposit is a skarn-type deposit occurring at the contact zone between intermediate-acidic magmatic rocks and carbonate rocks, the prospecting approach would necessarily focus on deploying exploration work around the intrusive bodies and carbonate rock contact zones, rather than seeking fault structures. However, the ore deposit under study does not exhibit characteristics of a skarn-type deposit. In the upcoming research work, we will fully leverage geochemical methods for ore deposits, analyzing the sulfur isotopes of ore metal sulfides, the C, H, and O isotopes of gangue minerals, ore fluid inclusions, and the geochemical characteristics of rock masses genetically related to the ore body, to comprehensively reveal the genesis and metallogenic process of this gold deposit. This will guide the prospecting work in the mine and its surrounding areas.

5. Conclusions

Based on previous research and the summary of this study, the following understandings are obtained:

1. The exposed strata in the mining area are primarily composed of Late Paleozoic and Early Mesozoic intermediate-acidic volcanic lava, volcanic tuff, and intermediate-acidic intrusive rocks, as well as a portion of Middle-Late Mesozoic sedimentary clastic rocks, indicating active tectonic-magmatic activity. The ore bodies are mainly hosted in intermediate volcanic lavas and volcanic tuffs, occurring in brittle shear structural fractures within the left-lateral strike-slip fault zone through hydrothermal filling and metasomatism. The ore bodies are gently dipping towards the south, distributed in a near-east-west direction along the fault zone, strictly controlled by the fault zone, and morphologically lens-shaped with local enlargement, narrowing, pinch-outs, reappearances, branching, and compositing characteristics. The ores exhibit granular structure, subhedral structure, porphyroclastic structure, and oriented crystalline texture, with structures such as disseminated, vein-like, and cataclastic breccia. The main ore minerals are pyrite, sphalerite, galena, and chalcopyrite, while the gangue minerals are mainly quartz, calcite, and dolomite. Gold mainly occurs as included gold or fissure gold within the crystal lattices and microfractures of minerals such as pyrite and sphalerite. The wall rock alteration can be broadly classified into: a mineralized alteration zone characterized by silicification and carbonatization; a near-ore wall rock alteration zone characterized by chloritization and sericitization; and a surface weathering alteration zone characterized by limonitization;

2. Based on the mineral assemblages and their genetic timing relationships, the mineralization can be divided into three stages: arsenopyrite-pyrite-dolomite-quartz (I), sphalerite-galena-chalcopyrite-calcite (II), and siderite (III), with the latter stages often overprinting the earlier ones, showing obvious cross-cutting and metasomatic phenomena;

3. It is believed that this deposit is a low-temperature hydrothermal filling-metasomatic gold deposit produced within a brittle shear zone. The tectonic activity during the Hercynian period and earlier caused widespread intermediate-basic magmatic activity in the region, which may have constituted the gold material basis and abundant hydrothermal fluids. During the Indosinian period, intense collision orogenesis in the study area was accompanied by intermediate-acidic volcanic magmatic activity, coinciding with regional tectonic transformation, forming a northwest-trending tectonic framework and compressive-shear to tensile fracture zones in the mining area, providing space for the ascent of hydrothermal fluids and the emplacement of ore bodies. The intermediate volcanic lavas and volcanic tuffs provided a chemical environment for hydrothermal metasomatism and the precipitation and deposition of gold

and gold-bearing minerals. In the late Indosinian period, intermediate-acidic porphyry bodies intruded, mixing with multiple episodes of volcanic hydrothermal fluids, continuously extracting and activating gold from earlier magmatic activity and gold carried by themselves. Under the background of regional compressive-shear stress, they ascended into the underpressured brittle shear zones, forming gold ore bodies through filling-metasomatic processes.

Author Contributions

Conceptualization, C.L.; methodology, C.L.; software, W.H., Y.Q., N.Y., Z.W., Y.X.; validation, C.L and D.Y.; formal analysis, C.L.; investigation, C.L.; resources, C.L.; data curation, C.L.; writing—original draft preparation, C.L.; writing—review and editing, C.L.; visualization, C.L.; supervision, C.L.; project administration, D.Y.; funding acquisition, D.Y. All authors have read and agreed to the published version of the manuscript.

Funding

"Research Project on Metallogenic Regularity and Metallogenic Prediction of the Sakai Gold Deposit in Vientiane, Laos" funded by Yunnan Land and Resources Vocational College.

Institutional Review Board Statement

Not applicable.

Informed Consent Statement

Not applicable.

Data Availability Statement

All data related to this research project belong to my university. Reasonable access to and consultation of the data for scientific research purposes are permitted. The data published in the paper are authentic experimental data and may be cited.

Conflicts of Interest

The authors declare no conflict of interest.

References

[1] Feng, Q.L., Chonglakmani, C., Helmcke, D., et al., 2005. Correlation of Triassic stratigraphy between the Simao and Lampang Phrae basins: Implications for the tectonopaleogeography of Southeast Asia. Journal of Asian Earth Sciences. 24, 777–785.

[2] Sone, M., Metcalfe, I., 2008. Parallel Tethyan sutures in mainland Southeast Asia: New insights for Palaeo Tethys closure and implications for the Indosinian orogeny. Comptes Rendus Geoscience. 340(2/3), 166–179.

[3] Metcalfe, I., 2013. Gondwana dispersion and Asian accretion: Tectonic and palaeogeographic evolution of eastern Tethys. Journal of Asian Earth Sciences. 66, 1–33.

[4] Burrett, C., Zaw, K., Meffre, S., et al., 2014. The configuration of Greater Gondwana: Evidence from LA ICPMS, U-Pb geochronology of detrital zircons from the Palaeozoic and Mesozoic of Southeast Asia and China. Gondwana Research. 26(1), 31–51.

[5] Qian, X., Feng, Q., Wang, Y., et al., 2016. Petrochemistry and tectonic setting of the Middle Triassic arc-like volcanic rocks in the Sayabouli area, NW Laos. Journal of Earth Science. 27(3), 365–377.

[6] Qian, X., Feng, Q., Yang, W., et al., 2015. Arc-like volcanic rocks in NW Laos: Geochronological and geochemical constraints and their tectonic implications. Journal of Asian Earth Sciences. 98, 342–357.

[7] Shi, M.F., Wu, Z.B., Liu, S.S., et al., 2019. Geochronology and petrochemistry of volcanic rocks in the Xaignabouli area, NW Laos. Journal of Earth Science. 30(1), 37–51.

[8] Kamvong, T., Zaw, K., Meffre, S., et al., 2014. Adakites in the Truong Son and Loei fold belts, Thailand and Laos: Genesis and implications for geodynamics and metallogeny. Gondwana Research. 26(1), 165–184.

[9] Manaka, T., Zaw, K., Meffre, S., et al., 2014. The Ban Houayxai epithermal Au-Ag deposit in the Northern Lao PDR: Mineralization related to the Early Permian arc magmatism of the Truong Son Fold Belt. Gondwana Research. 26(1), 185–197.

[10] Salam, A., Zaw, K., Meffre, S., et al., 2014. Geochemistry and geochronology of the Chatree epithermal gold-silver deposit: Implications for the tectonic setting of the Loei Fold Belt, Central Thailand. Gondwana Research. 26(1), 198–217.

[11] Leaman, P., Manaka, T., Jarical, K., et al., 2019. The geology and mineralization of the Long Chieng Track (LCT) subvolcanic Au-Ag-Cu-Pb-Zn deposit, Lao PDR. Ore Geology Reviews. 106, 387–402.

[12] Ren, J.S., Wang, Z.X., Chen, B.W., 1999. Viewing the Tectonics of China from a Global Perspective. Geological Publishing House: Beijing, China. pp. 9–19.

[13] Li, X.Z., Liu, C.J., Ding, J., 2004. Division of structural

units in the Greater Mekong Subregion. Sedimentary Geology and Tethys Geology. 24(4), 1–12.

[14] Wang, H., Lin, F.C., Li, X.Z., et al., 2015. Division of tectonic units and tectonic evolution in Laos and its adjacent areas. Geology in China. 42(1), 71–84.

[15] Zhao, Y.P., He, G.C., Lu, J.H., 2013. Geological characteristics and metallogenic regularity of gold metallogenic belts in Laos. Geological Review. 59, 295–296.

[16] Zhao, Y.P., He, G.C., Lu, J.H., 2013. Geological characteristics and metallogenic model of typical gold deposits in Laos. Mineral Resources and Geology. S1, 41–46.

[17] Zhu, Y.Z., Wu, J., Hu, J.J., et al., 2009. An Overview of Geology and Mineral Resources of Laos. Yunnan Science and Technology Press: Kunming, China. pp. 1–153.

[18] Liu, S.S., Yang, Y.F., Guo, L.N., et al., 2018. Tectonic characteristics and mineralization in Southeast Asia. Geology in China. 45(5), 863–889.

[19] Bunopas, S., 1981. Palaeogeographic History of Western Thailand and Adjacent Parts of Southeast Asia: A Plate Tectonic Interpretation. Geological Survey Professional Paper, 5, Special Issue 810 p, Bangkok.

[20] Bar, S.M., Maedonald, A.S., 1987. Nan River suture zone, northern Thailand. Geology. 15(10), 71–74.

[21] Hutchison, C.S., 1975. Ophiolites in Southeast Asia. Geological Society of America Bulletin. 86, 797–806.

[22] Intasopa, S.B., 1993. Petrology and geochronology of the volcanic rocks of the Central Thailand volcanic belt [PhD thesis]. Fredericton, Canada: University of New Brunswick. pp. 1–269.

[23] Intasopa, S.B., Dunn, T., 1994. Petrology and Sr-Nd isotopic systems of the basalts and rhyolites, Loei, Thailand. Journal of Southeast Asian Earth Sciences. 9(1/2), 167–180.

[24] Goldfarb, R.I., Taylor, R.D., Collins, G.S., et al., 2014. Phanerozoic continental growth and gold metallogeny of Asia. Gondwana Research. 25(1), 48–102.

[25] Gao, Y.L., Niu, Y.J., Liu, Z.Y., et al., 2017. Distribution characteristics and metallogenic prospects of gold resources in Laos. Modern Mining. 5, 27–32.

[26] Miao, L.C., Luo, Z.K., 1997. Evolution of ore-controlling faults in the Zhao-Ye Gold Belt of Jiaodong. Contributions to Geology and Mineral Resources Research. 1, 26–35.

[27] Ren, S.L., 1994. Study on ore-controlling structures of the Laowangzhai-Donggualin gold deposits in the Northern Ailaoshan Range. Mineral Deposits. 13, 43–44.

[28] Shi, M.F., Khin, Z., Liu, S.S., et al., 2021. Geochronology and petrogenesis of Carboniferous and Triassic volcanic rocks in NW Laos: Implications for the tectonic evolution of the Loei Fold Belt. Journal of Asian Earth Sciences. 208, 104661.